Motor current based force control of simple cable-driven parallel robots

Jonas Bieber, David Bernstein, Micha Schuster, Konrad Wauer, and Michael Beitelschmidt

Chair of Dynamics and Mechanism Design, Technische Universität Dresden, Germany
jonas.bieber@tu-dresden.de

Abstract. State of the art cable-driven parallel robots achieve high precision and reliability using a complex setup. The complexity results largely from the integration of force sensors which are omitted in the presented design. Instead, a motor current based approach is proposed to determine the cable forces. Therefore, methods are employed to compensate the cogging torque of the motor and frictional forces along the transmission path from the motor torque to the acting force at the platform. Despite the compensation, it is useful to reduce the overall frictional forces. Therefore, a gearless design scheme with a single pivoting pulley for cable guidance is realized. The proposed approach enables the application of advanced control methods for simple cable-driven robots.

Keywords: Cable-driven parallel robot · Force control · Motor current · Cogging compensation · Friction compensation · Gearless

1 Introduction

Advantages of cable-driven parallel robots are a large workspace, high achievable speeds and high payload. Intensive research in the last decades has lead to robots with high precision and reliability [17,11,4]. Many advanced approaches rely on a force or torque based control to stay within cable force limits and enable high pose control performance or haptic force feedback [7,10,9]. To determine and to control the acting forces, force sensors are used, by which however the system complexity is increased notably. This complexity is reflected in the number of mechanical and electrical components, as well as the effort and cost of integrating them into the system.

In order to make the technology of cable-driven robots accessible for a broader range of applications, reducing the complexity and costs is an important issue. The costs can be reduced by taking advantage of the increasing availability of inexpensive yet powerful components from the hobbyist sector such as single board computers and brushless motors. On the other hand, a high potential for a reduction of complexity can be found in omitting force sensors. To maintain a high control performance by force based control, the motor currents can be used to determine the forces acting on the robot platform. As a consequence, a setup with minimized friction and a model of the remaining friction and other disturbing effects is necessary, and will be presented in this paper.

2 Relationship between motor current and cable force

There is an approximately linear relationship between motor current and cable force acting on the platform. However, nonlinearities and discontinuities appear in the detailed consideration of the transmission path. These are described below.

2.1 From current to torque

For ideal electric motors, the proportional relation between the armature current i and the generated torque τ_0 is given with the motor dependent torque constant k_τ as

$$\tau_0 = k_\tau i \; . \tag{1}$$

For brushless motors with three phases, the torque generating motor current i corresponds to the quadrature current component i_q orthogonal to the rotor magnetic field. It can be obtained from the phase currents via direct-quadrature-zero transformation. Utilizing field oriented control the torque generating current i_q is set to the desired value. On real brushless motors, angle-dependent deviations from the linear relation in Eq. (1) occur. The main cause of these torque-ripples is the cogging phenomenon. It results from the non-constant interaction force between the permanent magnets on the rotor and the stator slots inside the motor. The cogging torque $\tau_\mathrm{c}(\varphi)$ leads to the mechanical output torque τ_m

$$\tau_\mathrm{m} = \tau_0 + \tau_\mathrm{c}(\varphi) \; . \tag{2}$$

This effect is independent of the motor current i and depends only on the motor angle φ, which results in a deterministic offset with

$$\tau_\mathrm{c}(\varphi) = \tau_\mathrm{c}(\varphi + 2\pi n) \;\; \text{with } n \in \mathbb{Z} \; . \tag{3}$$

Thus, at low load, cogging contributes a high proportion of the total torque τ_m, whereas its contribution decreases with higher loads. Furthermore, at high speeds, the system inertia reduces the impact of the effect. The magnitude of the cogging torque depends on the motor design, manufacturing variations and tolerances [5]. Therefore, the effect is in general more significant for inexpensive motors [14].

2.2 From motor torque to cable force

For the idealized transmission, the relationship between motor torque τ_m and cable force f holds

$$f = \nu \cdot \tau_\mathrm{m} \tag{4}$$

with the transmission ratio ν.

In reality, the load is transmitted via the motor, gearbox, winch and several other mechanical components as pulleys. Along the transmission path, additional

forces apply. Considering the most important effects, the resulting cable force f_{act} can be described as

$$f_{\mathrm{act}} = \nu \cdot \tau_{\mathrm{m}} - \nu \cdot J\ddot{\varphi} - \mathrm{sgn}(\dot{\varphi}) \cdot f_{\mathrm{f}} \,. \tag{5}$$

Accordingly, inertial forces apply depending on the motor acceleration $\ddot{\varphi}$. The inertias of all transmission path elements are represented by the total inertia J. The frictional force f_{f} depends on the direction of motion $\mathrm{sgn}(\dot{\varphi})$. Within the frictional force, three main components can be identified:

$$f_{\mathrm{f}} = f_{\mathrm{f,i}} + f_{\mathrm{f,l}}(\tau_{\mathrm{m}}) + f_{\mathrm{f,v}}(\dot{\varphi}) \tag{6}$$

The frictional force mainly results from losses in the bearings of the rotating components. It is composed of:

a) $f_{\mathrm{f,i}} = \text{const.}$: a constant frictional force that is independent of cable force and movement. It can be considered as internal friction caused by permanent normal forces on the bearings such as gravity and preloads.
b) $f_{\mathrm{f,l}} \approx \mu \cdot \nu\tau_{\mathrm{m}}$: a load dependent frictional force. Approximately, a linear dependency on the mechanical torque τ_{m} is assumed. A more precise approach as presented in [6] also takes into account the force change due to friction along the transmission path and the pose-dependent wrapping angles of the pulleys.
c) $f_{\mathrm{f,v}}(\dot{\varphi})$: a frictional force depending on the cable velocity, typically described as viscous friction.

While $f_{\mathrm{f,v}}$ and the inertial loads $J\ddot{\varphi}$ only occur during movements of system, $f_{\mathrm{f,i}}$ and $f_{\mathrm{f,c}}$ are also relevant in the static case. The dependence of friction on the direction of motion leads to a hysteresis effect. Therefore, a specific motor torque results in higher cable forces when uncoiling compared to coiling up the cable. This leads to a discontinuity in the relationship between motor torque and cable force. In reality, however, the discontinuous signum function in Eq. (5) is smoothened by elasticity effects.

3 Considerations for motor current based force control

The mechanical and electrical integration of accurate force sensors and A/D converters increases costs and complexity of advanced cable-driven robots. Furthermore, integrating the measured cable forces into cascaded force control loops leads to latencies due to signal processing [8]. In order to simplify force based control, under certain conditions, the cable force can be determined via the motor currents instead. The drawbacks of this current based force estimation are systematic deviations mainly caused by friction and cogging torque. These deviations can generally be described based on a simple propagation of uncertainty of the cable force from Eq. (5), which describes the deviation Δf of the acting cable force f_{act} from the desired cable force f_{des} at the platform as

$$\Delta f = f_{\mathrm{act}} - f_{\mathrm{des}} = \nu \cdot \Delta\tau_{\mathrm{m}} + \Delta f_{\mathrm{f}} + f_{\mathrm{res}} \,. \tag{7}$$

Since every uncompensated frictional force as well as every modeling error is incorporated in the term $\Delta f_\mathrm{f} = f_\mathrm{f} - f_\mathrm{comp}$, it is suitable to take measures to reduce the overall friction f_f in the setup and develop a model for the friction compensation with $f_\mathrm{comp} \approx f_\mathrm{f}$. On the other hand, the error torque $\Delta\tau_\mathrm{m}$ comprises the cogging torque τ_c that has to be compensated, as well as measurement errors of the current and motor parameter uncertainties. All residual effects are summarized in f_res. In the following, a robot design scheme and compensation methods to reduce the impact of cogging torque and friction are proposed.

3.1 Design

As mentioned above, it is crucial to minimize the effects of cogging and friction to maintain a high precision in the prediction of the cable force even in the presence of modeling errors or further unmodeled phenomena. Thus, to reduce the frictional force, a minimalistic design is beneficial. The consequences of this approach are discussed below.

Absence of a gearbox Typically, gearboxes are an integral part of the drive system design of cable-driven robots. Since high-torque motors are more expensive in general, gearboxes allow high cable forces using low-torque motors. But especially the use of gearboxes increases the frictional forces. As described in [16], the efficiency factor of gearboxes of up to 95% at nominal load descreases at low cable forces. In particular, the frictional force f_f resulting from friction in the gearbox can be higher than low actual cable forces [7]. Those low cables forces typically occur when uncoiling the cable, often combined with high velocities increasing the viscous frictional force $f_\mathrm{f,v}$.

Due to the design goal of reducing the frictional force f_f as much as possible, gearboxes are not used. Instead, there is a direct coupling between the motor shaft and the winch.

Simple cable guidance For cable-driven robots, cable guidance is used to ensure a controlled coiling of the cable on the drum. A cable guidance with multiple redirections of the cable allows a flexible positioning of the drive units, in addition. Typically, for this purpose mechanisms using pulleys or eyelets are deployed. The mechanical force loss inside of pulleys due to friction is about 3% [16] and is likely even higher in eyelets. Therefore, especially a cable guidance with many redirections of the cable leads to increased mechanical losses.

Figure 1 shows a setup where a single pivoting pulley is sufficient to achieve a single-layer coiling. Since the winch consists solely of a drum on a shaft without dedicated cable guidance, this imposes restrictions on the placement of the winch, especially regarding the deflection angle ϑ. The angle ϑ is defined relative to the pivoting pulley and increases when coiling up the cable. To prevent cable twisting and allow single-layer coiling, the angle ϑ has to meet the limits:

$$\vartheta_\mathrm{min} \leq \vartheta \leq \vartheta_\mathrm{max} \,. \tag{8}$$

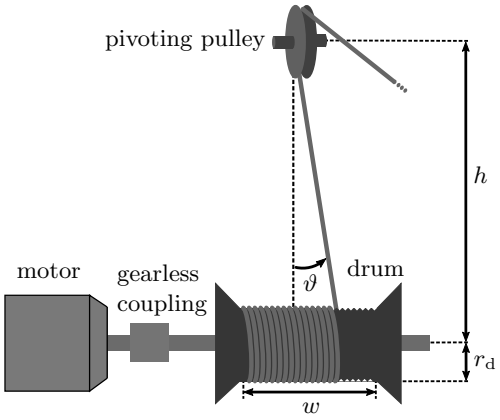

Fig. 1. Basic design of the drive unit and the simple cable guidance using a simple pivoting pulley

The absolute value of the maximum deflection angle is typically larger than the absolute value of the minimum ($|\vartheta_{\max}| > |\vartheta_{\min}|$) due to the support of the already coiled cable. The absolute value of the minimum deflection angle $|\vartheta_{\min}|$ can be increased by a guiding helical groove on the drum. The angle restrictions result in a maximum width $w_{\max}$ of the drum of

$$w_{\max} = h \cdot (\tan(\vartheta_{\max}) + \tan(|\vartheta_{\min}|)) \tag{9}$$

for large distances $h \gg r_{\mathrm{d}}$ between pulley and drum.

Radius of the drum In the simplified setup, the radius of the drum r_{d} plays an important role. Since no gearbox is used, the transmission $\nu = \frac{1}{r_{\mathrm{d}}}$ only depends on the radius r_{d} of the drum. Therefore, a large drum radius can be used to minimize the effect of the torque errors $\Delta\tau_{\mathrm{m}}$ by reducing its scale factor ν in Eq. (7). On the other hand, an enlarged drum radius leads to higher motor torques for the same cable force and thus reduces the relative torque errors $\Delta\tau_{\mathrm{m}}/\tau_{\mathrm{m}}$ due to the load-independent cogging torque τ_{c}. As a side effect, a high drum radius increases the maximum usable cable length. With a given maximum drum width $w_{\max}$ (Eq. (9)) and diameter of the cable d_c, the maximum cable length that can be coiled is

$$\Delta\ell_{\max} = 2\pi r_{\mathrm{d}} \frac{w_{\max}}{d_{\mathrm{c}}} \,. \tag{10}$$

On the other hand, typical applications for cable-driven robots require relatively high cable forces and rather lower speeds. Thus, with a large radius r_{d} more expensive high-torque motors are needed. The proposed simple design scheme therefore requires careful adjustment of the distance between winch and pulley,

the drum radius and the maximum motor torque. Due to their high torque-density, especially brushless outrunner motors are suitable. Here, appropriate hobbyist motors are available at moderate price.

3.2 Cogging compensation

Besides frictional forces, the second source of disturbances that has to be minimized is cogging. Figure 2 shows the effect of cogging on the cable force for the prototype presented in section 4.1. The quasi-static cable force at the winch is measured with a force sensor over one motor revolution for a constant motor current i_q at very low speed with about one rotation per minute.

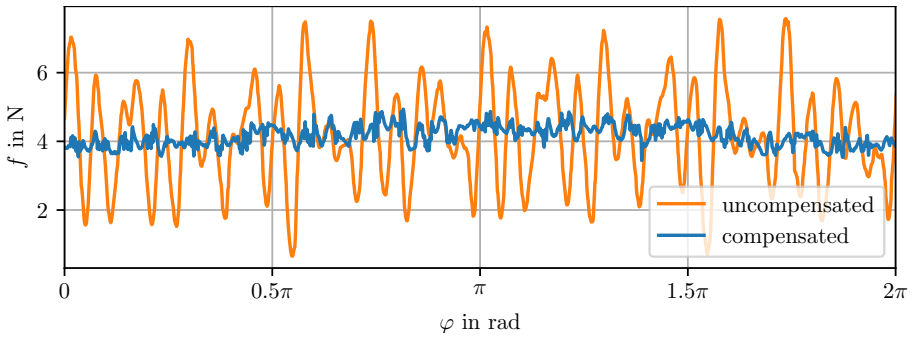

Fig. 2. Quasi-static cable force f directly behind the winch over one motor revolution with and without cogging compensation for $\tau_\mathrm{des} = \mathrm{const}$

Since the cogging torque occurs systematically and depends only on the rotation angle of the motor, it can be largely compensated in the motor controller. For this purpose, the desired torque τ_des is adjusted with an offset $\tau_\mathrm{comp} \approx \tau_\mathrm{c}$ to cancel out the cogging torque

$$\tau_\mathrm{set} = \tau_\mathrm{des} - \tau_\mathrm{comp}(\varphi) \; . \tag{11}$$

A method to find this angle-dependent offset without requiring external measurement equipment is proposed in [14]. Here, the offset torque $\tau_\mathrm{comp}(\varphi)$ is determined as the motor torque required to maintain the position of the unloaded motor. The method is implemented as a feature in the firmware of the *ODrive* motor controllers [1] that are used in the experimental setup. Figure 2 also shows the improvements achieved by the anti-cogging feature. The fluctuations of the motor torque can be reduced noticeably.

3.3 Friction compensation

In general, to compensate the relevant frictional forces, all contributions between platform and sensors for force determination have to be considered. For systems

where the cable force is measured at the winch or pulleys, friction estimation and compensation methods are proposed in [6,10,12,13]. If the force determination is based on the motor current as proposed in section 3.1, the friction in the motor and winch bearings has to be considered as well. In the following, a method is proposed to compensate main parts of the frictional force f_f. As mentioned in section 2.2, the resulting friction along the whole transmission path is analyzed rather than examining the individual components bottom-up.

Since friction acts against the direction of motion, it can be calculated from the measured force difference $f_\mathrm{act,diff} = f_\mathrm{act,uncoil} - f_\mathrm{act,coil}$ between the cable forces during coiling $f_\mathrm{act,coil}$ and uncoiling $f_\mathrm{act,uncoil}$ while the same desired force f_des is applied. Figure 3 shows the resulting cable forces in relation to the desired cable force f_des measured on the prototype (see section 4.1).

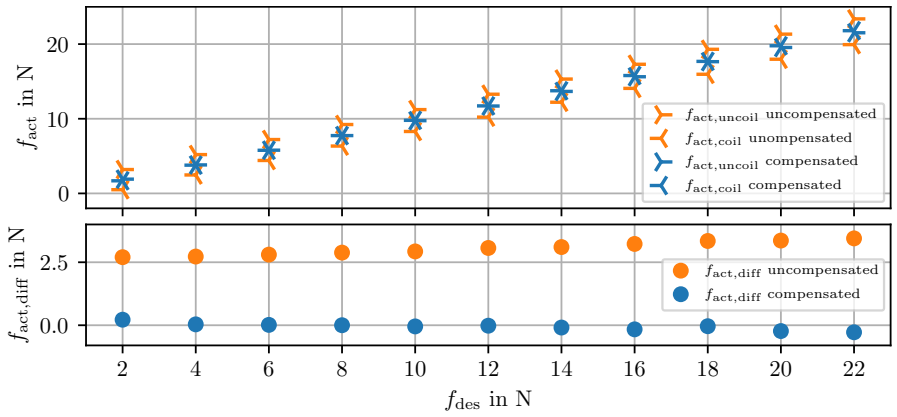

Fig. 3. Cable force f_act and cable force difference $f_\mathrm{act,diff}$ between coiling and uncoiling, with and without friction compensation

For the measurement, the cable force f_act is determined using a force sensor close to the center of the workspace. It thereby includes all friction components from motor, winch and pulley. The force sensor is manually moved in direction of the cable neutral axis while f_des is hold constant. To be able to neglect the influence of cogging, measurements are averaged over one motor revolution. Since the force sensor is moved at very low and constant speed, the cable force components resulting from inertia J and velocity-dependent friction $f_\mathrm{f,v}$ (see Eq. (5)) can be neglected. Under the corresponding assumption of a static case, it holds

$$f_\mathrm{f} = f_\mathrm{f,i} + \mu f_\mathrm{des} = \frac{f_\mathrm{act,diff}}{2} \,. \tag{12}$$

The frictional force is calculated from the cable force difference in the uncompensated case. From the measurement the parameters $f_\mathrm{f,i} \approx 1.3\,\mathrm{N}$ and $\mu \approx 0.018$ are approximated.

After compensating the friction based on Eq. (12), the lower part of Figure 3 shows the cable force difference $f_{\mathrm{act,diff}}$ for the uncompensated case and a compensation based on Eq. (12). It is shown that velocity independent frictional forces are compensated well.

To compensate the frictional force, the set cable force f_{set} is calculated as

$$f_{\mathrm{set}} = f_{\mathrm{des}} + f_{\mathrm{comp}} \, . \tag{13}$$

Apart from direction changes of the cable motion $\mathrm{sgn}(\dot{\varphi})$, f_{comp} corresponds to the frictional force f_{f}. However, to avoid control instability resulting from the discontinuity of the frictional force when changing the direction of motion, the frictional force is integrated in the compensational force as

$$f_{\mathrm{comp}} = f_{\mathrm{f}} \cdot \mathrm{sgn}(\dot{\varphi}) + (f_{\mathrm{comp},0} - f_{\mathrm{f}} \cdot \mathrm{sgn}(\dot{\varphi})) \cdot e^{-\frac{\sigma}{f_{\mathrm{f}}} \cdot |\varphi - \varphi_0|} \tag{14}$$

instead of using a signum function as in Eq. (5). When the direction of motion changes, the variables $\varphi_0 = \varphi$ and $f_{\mathrm{comp},0} = f_{\mathrm{comp}}$ are set. The parameter σ determines how stiff a direction change reverses the frictional force. At the time of the paper submission it is set based on empirical investigation.

The approach implies the consideration of the system elasticity using the Dahl model [2] as already used in [6] and [12] for cable-driven robots. However, systematical errors occur when the cable force is calculated in a reactive manner from the encoder values. Trajectory based prediction of direction changes might minimize those errors.

As a further approach, the dynamic forces in the Eqs. (5) and (6) can be taken into account. The current procedure requires the use of a force sensor for calibration. Possibilities for sensorless identification of friction parameters are part of future research.

4 Prototype

A cable-driven parallel robot prototype has been developed at the TU Dresden in the project *RopeBot*. In the following, the hardware used and the implemented control loop are described and a measurement on a trajectory is shown.

4.1 Hardware

The prototype is a redundant, suspended setup with 8 cables and 6 degrees of freedom (see Figure 4). The design corresponds to the simple scheme presented in section 3.1. Two drive units, consisting of a motor and winch, are mounted in a common modular motor block. A single *ODrive* motor controller controls both brushless motors of a motor block. Apart from the 3D-printed drums and pulleys made of PETG plastic, only mechanical standard parts are used to assemble the motor blocks and pivoting pulleys. Those are attached to an aluminum frame.

With a maximum motor torque of $\tau_{\mathrm{max}} = 3.86\,\mathrm{Nm}$ and a drum radius of $r_{\mathrm{d}} = 30\,\mathrm{mm}$, the maximum cable force is $f_{\mathrm{act,max}} = 128\,\mathrm{N}$. Further design details

Fig. 4. Prototype of a spacial redundant cable-driven robot

are summarized in table 1. For a future application with an installation space of about $6\,\mathrm{m} \times 6\,\mathrm{m} \times 4\,\mathrm{m}$, the drums are designed with the specified width w providing a distance $h \geq 2\,\mathrm{m}$.

Table 1. Components and parameters of the prototype

Cable:	*Dyneema*® 1 mm	**Frame:**	$2\,\mathrm{m} \times 1.7\,\mathrm{m} \times 1.2\,\mathrm{m}$
Control computer:	*Raspberry Pi 4 Model B*	**Platform:**	$0.4\,\mathrm{m} \times 0.4\,\mathrm{m} \times 0.12\,\mathrm{m}$
Motor:	*ODrive D6374 150KV*		5.1 kg
Motor controller:	*ODrive V3.6*	**Drum:**	$r_\mathrm{d} = 30\,\mathrm{mm}$
Encoder:	*CUI Devices AMT-102*		$w = 80\,\mathrm{mm}$

4.2 Control

Figure 5 shows the implemented control scheme. The estimated pose of the platform $\mathbf{p}_\mathrm{est}$ is determined from the motor angles $\boldsymbol{\varphi}$ using iterative forward kinematics. Starting with a known pose, the platform pose is observed through an iterative scheme using Newton-Raphson algorithm [3]. The initial pose is estimated with the interval analysis inspired technique given in [16].

A desired wrench $\mathbf{w}_\mathrm{des}$ is calculated in the PID controller from the deviation $\mathbf{e} = \mathbf{p}_\mathrm{des} - \mathbf{p}_\mathrm{est}$ between the desired pose and the actual pose. This is distributed to the cable forces $\mathbf{f}_\mathrm{des}$ using the improved closed-form solution [15]. Although minimum cable forces are targeted, it is ensured that the cable force is kept within the limits $1\,\mathrm{N} \leq f_\mathrm{des} \leq 100\,\mathrm{N}$.

Using the relationships described in section 2.2 and the friction compensation from section 3.3, the motor torques $\boldsymbol{\tau}_\mathrm{des}$ are calculated from the cable forces and

transferred to the *ODrive* motor controllers. The motor controllers calculate the desired motor current i_q according to section 2.1 and the adjusted torque according to the cogging compensation in section 3.2. In a decentralized cascaded control loop, the motor voltages of the three phases are adjusted by field-oriented control.

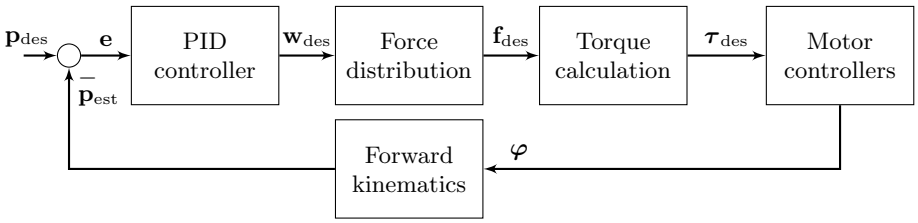

Fig. 5. Diagram of the control loop

4.3 Experimental Validation

The control of cable forces via motor currents is tested using a simple trajectory. Starting from a central point in the workspace, the platform performs a linear, translational back and forth movement. For a single cable, the motor angle φ and the desired cable force f_des are recorded. The actual cable force f_act is measured by a force sensor simultaneously. The results are shown in Figure 6.

In measurements of the uncompensated case, a mean absolute deviation of $\Delta f_\mathrm{mean} = |f_\mathrm{act} - f_\mathrm{des}|_\mathrm{mean} = 2.37\,\mathrm{N}$ occurs. With compensation of friction and cogging, the mean absolute deviation of $\Delta f_\mathrm{mean} = 0.57\,\mathrm{N}$ is reduced by more than a factor of 4. Deviations mainly occur when the direction of motion changes at about 2.2 s and 6.4 s. This results from not considering inertia forces at the transmission path and from the reactive behavior of the Dahl implementation in Eq. (14).

5 Conclusion

The general possibility to set the cable forces via the motor currents is shown for cable-driven robots. The accuracy of the cable force prediction can be notably improved by modeling and compensating cogging and friction, which are the dominant disturbance effects.

For further improvement, the introduced model based feedforward control allows to compensate inertial forces and to predict changes of the cable motion direction improving the implemented Dahl model. Methods for determining and compensating viscous friction and the wrapping-angle-dependency of the pulley friction are also conceivable in the future.

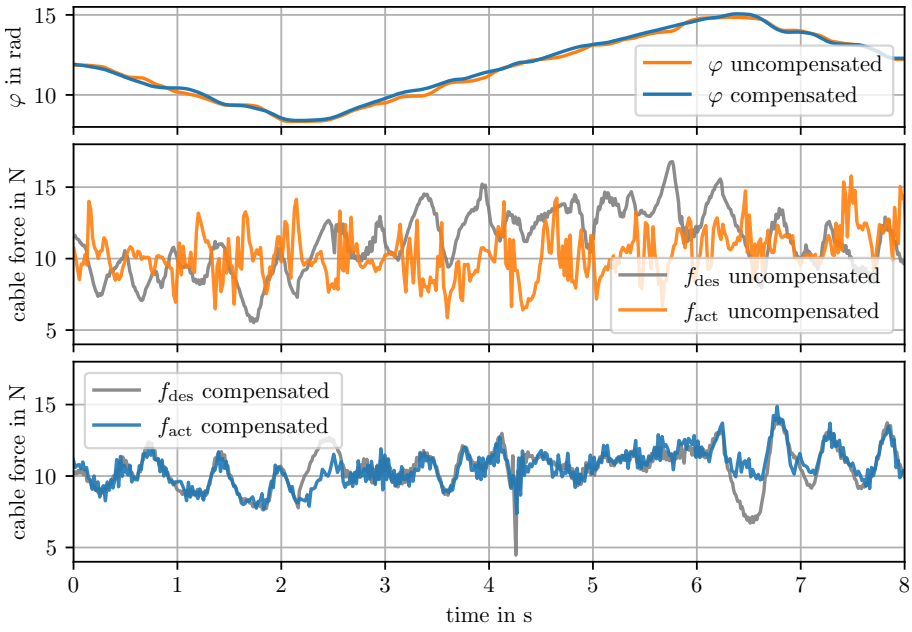

Fig. 6. Recorded motor angles φ and cable forces (desired f_{des} and measured f_{act}) without and with friction and cogging compensation for a single cable at an exemplary platform trajectory

Nevertheless, the achieved cable force accuracy of the presented approach can already be sufficient for many applications. It is shown that force based control is possible using a simple design approach without force sensors. A basic requirement is to use a gearless drive unit and a minimum number of pulleys for the cable guidance. The proposed design helps to reduce costs for cable-driven robots in general. Due to the determination of the cable forces, advanced control schemes are still deployable.

References

1. ODrive Firmware. ODrive Robotics (Mar 2021), `https://github.com/odriverobotics/ODrive`
2. Dahl, P.R.: A Solid Friction Model:. Tech. rep., Defense Technical Information Center, Fort Belvoir, VA (May 1968). https://doi.org/10.21236/ADA041920
3. Fang, S.: Design, Modeling and Motion Control of Tendon-Based Parallel Manipulators. No. 1076 in Fortschritt-Berichte VDI Reihe 8, Mess-, Steuerungs- Und Regelungstechnik, VDI-Verl, Düsseldorf (2005)
4. Hiller, M., Fang, S., Mielczarek, S., Verhoeven, R., Franitza, D.: Design, analysis and realization of tendon-based parallel manipulators. Mechanism and Machine Theory **40**(4), 429–445 (Apr 2005). https://doi.org/10.1016/j.mechmachtheory.2004.08.002

5. Islam, M.S., Islam, R., Sebastian, T., Chandy, A., Ozsoylu, S.A.: Cogging Torque Minimization in PM Motors Using Robust Design Approach. IEEE Transactions on Industry Applications **47**(4), 1661–1669 (Jul 2011). https://doi.org/10.1109/TIA.2011.2154350
6. Kraus, W., Kessler, M., Pott, A.: Pulley friction compensation for winch-integrated cable force measurement and verification on a cable-driven parallel robot. In: 2015 IEEE International Conference on Robotics and Automation (ICRA). pp. 1627–1632 (May 2015). https://doi.org/10.1109/ICRA.2015.7139406
7. Kraus, W.: Force Control of Cable-Driven Parallel Robots. No. 49 in Stuttgarter Beiträge Zur Produktionsforschung, Fraunhofer Verlag, Stuttgart (2016)
8. Kraus, W., Schmidt, V., Rajendra, P., Pott, A.: System identification and cable force control for a cable-driven parallel robot with industrial servo drives. In: 2014 IEEE International Conference on Robotics and Automation (ICRA). pp. 5921–5926. IEEE, Hong Kong, China (May 2014). https://doi.org/10.1109/ICRA.2014.6907731
9. Lamaury, J., Gouttefarde, M.: Control of a large redundantly actuated cable-suspended parallel robot. In: 2013 IEEE International Conference on Robotics and Automation. pp. 4659–4664 (May 2013). https://doi.org/10.1109/ICRA.2013.6631240
10. Lamaury, J., Gouttefarde, M., Chemori, A., Herve, P.E.: Dual-Space Adaptive Control of Redundantly Actuated Cable-Driven Parallel Robots. In: Proceedings of the ... IEEE/RSJ International Conference on Intelligent Robots and Systems. IEEE/RSJ International Conference on Intelligent Robots and Systems. pp. 4879–4886 (Nov 2013). https://doi.org/10.1109/IROS.2013.6697060
11. Lamaury, J., Gouttefarde, M., Michelin, M., Tempier, O.: Design and Control of a Redundant Suspended Cable-Driven Parallel Robots. In: Lenarcic, J., Husty, M. (eds.) Latest Advances in Robot Kinematics. pp. 237–244. Springer Netherlands, Dordrecht (2012). https://doi.org/10.1007/978-94-007-4620-6_30
12. Otis, M., Nguyen-Dang, T., Laliberté, T., Ouellet, D., Laurendeau, D., Gosselin, C.: Cable tension control and analysis of reel transparency for 6-DOF haptic foot platform on a cable-driven locomotion interface. International Journal of Electrical, Computer and Systems Engineering **3**, 16–29 (Jan 2009)
13. Piao, J., Kim, E.S., Choi, H., Moon, C.B., Choi, E., Park, J.O., Kim, C.S.: Indirect Force Control of a Cable-Driven Parallel Robot: Tension Estimation using Artificial Neural Network trained by Force Sensor Measurements. Sensors **19**(11), 2520 (Jan 2019). https://doi.org/10.3390/s19112520
14. Piccoli, M., Yim, M.: Cogging Torque Ripple Minimization via Position Based Characterization. In: Robotics: Science and Systems X. Robotics: Science and Systems Foundation (Jul 2014)
15. Pott, A.: An Improved Force Distribution Algorithm for Over-Constrained Cable-Driven Parallel Robots. In: Computational Kinematics, vol. 15, pp. 139–146. Springer Netherlands, Dordrecht (2014)
16. Pott, A.: Cable-Driven Parallel Robots: Theory and Application. Springer, Heidelberg (2018)
17. Pott, A., Mütherich, H., Kraus, W., Schmidt, V., Miermeister, P., Verl, A.: IPAnema: A family of Cable-Driven Parallel Robots for Industrial Applications. In: Cable-Driven Parallel Robot. Mech. Mach. Sci., vol. 12, pp. 119–134 (Jan 2013). https://doi.org/10.1007/978-3-642-31988-4_8